

Magnetic properties of NpGa₂ and NpSi₂

I. Yaar, S. Fredo, and J. Gal

*Department of Nuclear Engineering, Ben-Gurion University of the Negev, 84105 Beer-Sheva, Israel
and Nuclear Research Center-Negev (NRCN), P.O. Box 9001, 84190 Beer-Sheva, Israel*

W. Potzel and G. M. Kalvius

Physik-Department E15, Technische Universität München, D-8046 Garching, Federal Republic of Germany

F. J. Litterst

Institut für Metallphysik, Technische Universität Braunschweig, D-3000 Braunschweig, Federal Republic of Germany

(Received 24 June 1991; revised manuscript received 31 October 1991)

The magnetic and electronic properties of NpGa₂ and NpSi₂ were studied by Mössbauer as well as ac and dc magnetization techniques. NpGa₂ orders ferromagnetically at $T_C = 55(5)$ K with a Np-ion ordered moment of $\mu_{\text{ord}} = 2.39\mu_B$, which coincides with the value of the saturation moment μ_{sat} . The paramagnetic effective moment is $\mu_{\text{eff}} = 2.6\mu_B$. The Mössbauer isomer shift (IS) of NpGa₂ is +15.2 mm/sec relative to NpAl₂, indicating a Np³⁺ charge state. NpSi₂ has an IS of +7.9 mm/sec and orders ferromagnetically at $T_C = 48(5)$ K with $\mu_{\text{ord}} = 1.1\mu_B$, whereas $\mu_{\text{sat}} \approx 0.8\mu_B$. The paramagnetic effective moment is $\mu_{\text{eff}} = 2.1\mu_B$. A comparison of our data with the results for other NpX₂ ($X = \text{Al, As, Sb, Te}$) compounds indicates that NpGa₂ is a localized 5*f*-electron system, whereas in NpSi₂ the 5*f* electrons are partially delocalized. We show that at present the magnetic properties of the NpX₂ compounds cannot be consistently explained within the conventional crystal-field picture nor by taking into account hybridization dressing or using local-spin-density models.

I. INTRODUCTION

The NpX₂ ($X = s, p$ -electron ligand) intermetallic compounds exhibit puzzling changes in their crystallographic structures which are accompanied by large variations in their magnetic properties. The NpX₂ compounds crystallize in cubic Laves phase ($Fd\bar{3}m$), tetragonal ThSi₂-type ($I4_1/amd$), tetragonal Fe₂As-type ($P4/nmm$), and hexagonal AlB₂-type ($P6/mmm$) structures. NpSb₂ forms the orthorhombic LaSb₂ structure. The Np-Np spacing in the noncubic NpX₂ phases is about 4 Å, and, by the Hill criterion,¹ these compounds should all be magnetically ordered. In the present systems, this expectation is generally confirmed experimentally except for NpTe₂, which remains magnetically unordered down to 1.2 K. The magnetic behavior can be attributed to the sensitivity of spatial distribution of the 5*f*-electron wave functions to anisotropic hybridization with nearest-neighbor orbitals especially in a noncubic environment.² Recently it has been claimed that orbitally driven anisotropic hybridization leads to "crystal-field dressing" and a local magnetic moment could develop.²⁻⁴ Particularly, unfilled *s* and *p* bands of the appropriate symmetry near the Fermi energy mix with 5*f* crystal-field levels of the same symmetry, causing hybridization dressing of the local Np 5*f* levels.² Anisotropic hybridization may give rise to a coupling between orbital moments establishing magnetic order and an effective crystal-field splitting. This results in a fine structure in the 5*f* bands. Thus, orbital moments are observed even in highly itinerant-electron systems.^{3,5} On the other hand, anisotropic hybridization may cause a suppression of the magnetic moment, as, for

example, in CeTe and PuTe as described in Ref. 2. We shall discuss the magnetic behavior of the NpX₂ ($X = \text{Al, As, Si, Ga, Sb, Te}$) intermetallics in terms of this approach reviewed in Refs. 2 and 3.

From the Mössbauer isomer shift (IS) data, we argue that the Np ion in this family could be close to 3+ charge state. The hybridization dressing of the crystalline-electric-field (CEF) states introduces a complex level structure that cannot consistently be described by presently available models.

II. EXPERIMENTAL

NpGa₂ was prepared by arc melting stoichiometric amounts of neptunium and gallium in a dry argon atmosphere. X-ray- (Guinier) diffraction patterns showed that the sample consisted of a single hexagonal AlB₂-type (space group $P6/mmm$) phase with the lattice parameters $a = 4.259(3)$ Å, $c = 4.077(3)$ Å, in good agreement with the values given previously.⁶ The sample was powdered and sealed in an aluminum container for the Mössbauer experiments, and in a highly pure plastic container⁷ for the magnetization measurements.

NpSi₂ was prepared by a similar technique. The phase obtained also contained $\approx 10\%$ of NpSi₃. NpSi₃ does not order magnetically down to 4 K and thus contributes a single absorption line of a different IS which was taken into account when evaluating the Mössbauer spectra. NpSi₂ crystallizes in a tetragonal structure ($I4_1/amd$) with lattice parameters $a = 3.968(6)$ Å, $c = 13.715(20)$ Å.

²³⁷Np 60-keV Mössbauer transmission experiments were carried out between 4.2 and 60 K in a conventional

variable-temperature cryostat.⁸ The Mössbauer source was ²⁴¹Am (6%) in the Th metal matrix of full width at half maximum (FWHM) of 1.8 mm/sec. The dc magnetization measurements were performed with a vibrating sample magnetometer. The ac susceptibility results were obtained with our low-field (≈ 8 G), triple-coil susceptometer, which is described elsewhere.⁹

III. RESULTS

A. NpGa₂

The dc and ac susceptibilities of NpGa₂ between 20 and 100 K are shown in Figs. 1(a) and 1(b). The dc magnetization as well as the cusp at about 56(3) K are indicative of a ferromagnetic transition at this temperature (T_C). The reciprocal susceptibility at elevated temperatures [inset Fig. 1(a)] shows a Curie-Weiss behavior in the temperature range 150–230 K with a paramagnetic effective moment of $\mu_{\text{eff}} = [2.6(2)]\mu_B$ and a paramagnetic Curie-Weiss temperature $\Theta \approx 78$ K. Below 100 K, the effective moment increases slightly, a phenomenon we attribute to crystal distortions similar to that observed in UGa₂.¹⁰ This feature will be discussed below.

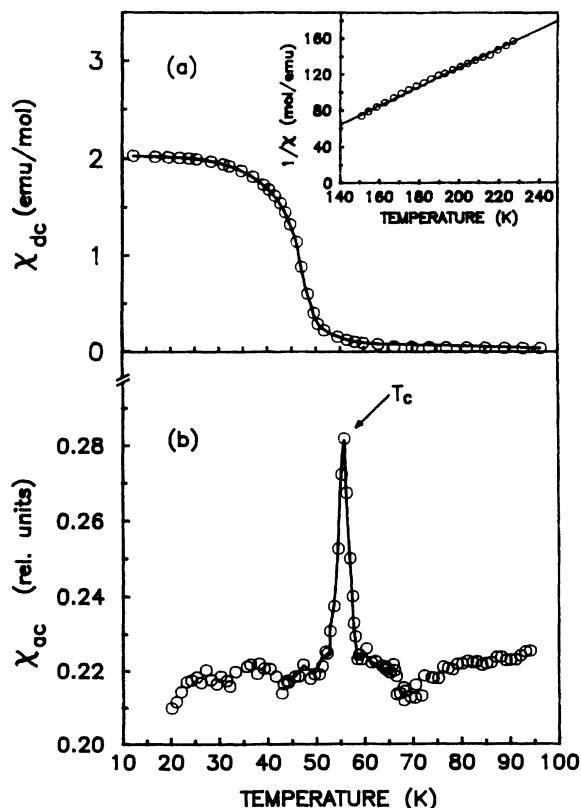


FIG. 1. (a) dc magnetization of NpGa₂ as function of temperature at an applied magnetic field of 0.3 T. The reciprocal susceptibility data at elevated temperatures are inserted. (b) ac susceptibility of NpGa₂ as function of temperature indicating a ferromagnetic transition at $T_C = 55(2)$ K.

The magnetization versus applied magnetic fields at 4.2 K is shown in Fig. 2. Saturation seems to be reached only above 1 T. Since very large anisotropy is dominant for actinide ferromagnets (except for highly itinerant ferromagnets), strong magnetocrystalline anisotropy should be taken into account. If we assume that, indeed, saturation has been achieved, and similar to the isostructural UGa₂,^{11,12} the hexagonal *c* direction is the magnetic easy axis, the relation between the saturation moment (μ_{sat}) and the saturation moment derived from the saturation magnetization experimental data (external applied field extrapolated to $B \rightarrow \infty$) of a powder sample (μ_{powder}) is given by $\mu_{\text{sat}} \approx 2\mu_{\text{powder}}$.¹³ Thus, for NpGa₂, a saturation moment of $\mu_{\text{sat}} = [2.4(3)]\mu_B$ per Np is obtained.

Typical ²³⁷Np Mössbauer absorption spectra of NpGa₂ in the temperature region between 4.2 and 50 K are shown in Fig. 3. Magnetically split patterns are observed below 50 K, indicating magnetic order of the Np moments. The hyperfine field at 4.2 K is $B_{\text{hf}} = 525(10)$ T, which corresponds to an ordered Np moment of $\mu_{\text{ord}} = [2.39(10)]\mu_B$.¹⁴ This result is in good agreement with the saturation moment derived from the dc magnetization measurements and close to the free-ion value.

The normalized magnetizations, as derived from the dc magnetization and the Mössbauer hyperfine fields for NpGa₂, are depicted in Fig. 4(a). Although the dc data are systematically somewhat lower than the Mössbauer data, their general behavior is the same. The discrepancy between the Brillouin curves and the experimental data could indicate a possible biquadratic contribution.

B. NpSi₂

dc and ac susceptibilities of NpSi₂, shown in Figs. 5(a) and 5(b), indicate that this compound orders ferromagnetically below $T_C \approx 48(3)$ K. The normalized magnetization displayed in Fig. 4(b) agrees with a Brillouin curve for $J=1$. The ordering temperature was further confirmed by a Mössbauer thermal scan measurement

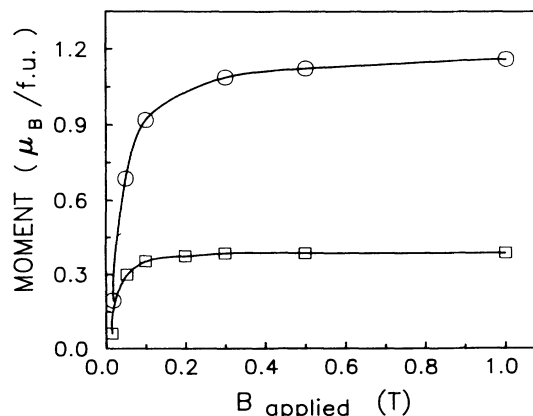


FIG. 2. dc magnetization of NpGa₂ (○) and NpSi₂ (□) (powder samples) vs the applied magnetic field at 4.2 K. The determination of μ_{sat} from the present data for powder samples is explained in the text.

and is compared in Fig. 5(c). Notable is the high agreement between the three techniques in determination of T_C . From the Mössbauer Zeeman pattern at 4.2 K shown in Fig. 6, a magnetic hyperfine field of $B_{\text{hf}}=244(10)$ T is derived. This corresponds to an ordered moment of $\mu_{\text{ord}}=[1.10(1)]\mu_B$ at the Np ion. The isomer shift of NpSi₂ is $+7.9(5)$ mm/sec. The variation of the magnetic moment of the NpSi₂ powder sample under applied magnetic field is depicted in Fig. 2. It seems that saturation is already reached above 0.3 T. A saturation moment $\mu_{\text{sat}}=[0.8(1)]\mu_B$ was obtained by extrapolation using similar arguments as for NpGa₂.

In conclusion, our measurements on NpSi₂ show discrepancies between the paramagnetic effective moment $\mu_{\text{eff}}=[2.15(5)]\mu_B$ [see inset in Fig. 5(a)] and μ_{ord} and μ_{sat} . In Table I, we summarize our experimental results on these two compounds and compare them with other intermetallics of the NpX₂ family. Within the systematics of the Mössbauer IS (Ref. 15) (see discussion) together with the experimental values of the paramagnetic effective moments (μ_{eff}) given in Table I, the Np ions in the NpX₂ intermetallics could be claimed to be close to the formal 3+ charge state. We will further discuss this

problem below in general and separately for each NpX₂ compound.

IV. DISCUSSION

The electronic and magnetic properties of the NpX₂ intermetallics sequenced according to their isomer shifts relative to NpAl₂ are compared in Table I. It has been pointed out previously that, for Np nonmetallic compounds, five distinct IS groups are identified corresponding to their $5f^n$ ($n=0,1,2,3,4$) Np charge states. The separations between the groups exceeds 20 mm/sec and are due to the strong shielding of the s electrons by the $5f$ electrons.¹⁵ This demonstrates the major role of the shielding phenomenon in establishing the IS. However, the small variation of the IS within each group (charge state) is often explained by the covalency of the chemical bond which may include s -, p -, and d -electron densities pumped from the ligand by the Np $5f$ core, affecting the s -electron density at the Np nucleus directly, or by smaller additional shielding effects. This phenomenon of co-

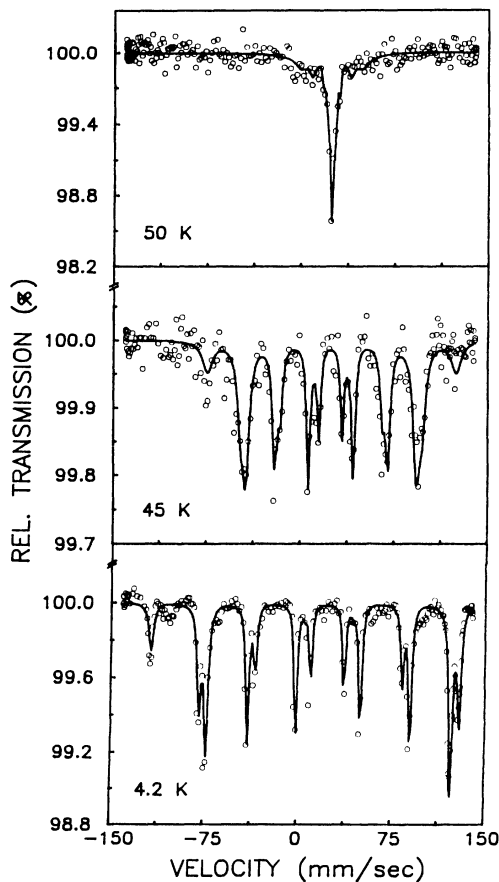


FIG. 3. ²³⁷Np Mössbauer absorption spectra of NpGa₂ at various temperatures. The Mössbauer source was ²⁴¹Am(Th).

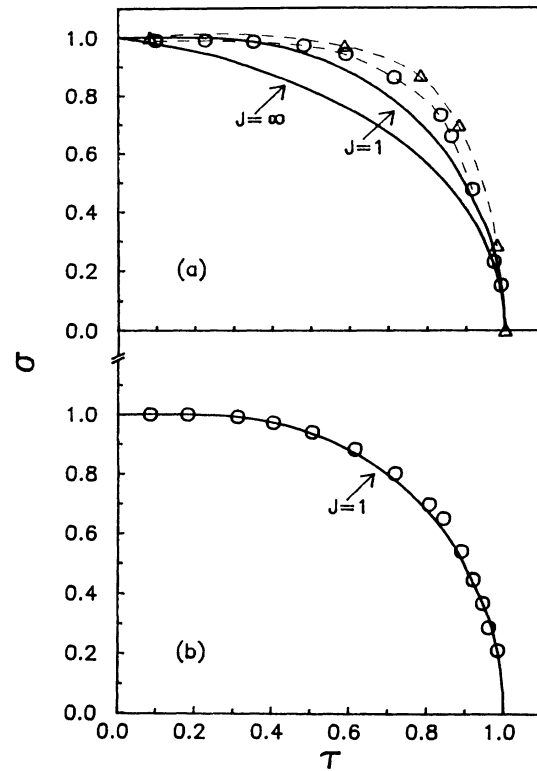


FIG. 4. (a) Normalized magnetization of NpGa₂ derived from Mössbauer (\circ) and dc magnetization (\triangle). The dashed lines are intended as a guide to the eye. The solid lines represent the Brillouin function for $J=1$ and ∞ . (b) Normalized magnetization of NpSi₂ derived from dc magnetization. The solid line represents the Brillouin function for $j=1$.

valent electrons in insulators¹⁶ is similar to hybridization of band electrons in metallic compounds.¹⁷

Experimentally, shielding effects can be detected primarily by the Mössbauer isomer shift technique providing a unique tool for studies of the $5f$ covalency as well as hybridization. Indeed, covalent effects can be observed for Np^{4+} through Np^{7+} , with the exception of Np^{3+} for which the $5f$ shielding is already so high that the IS of all nonmetallic Np^{3+} compounds falls within a narrow region of ± 0.5 mm/sec at $+38$ mm/sec.¹⁵ Therefore, in metallic systems also having a Np-ion close to a formal $3+$ charge state, the conduction s electrons are also high-

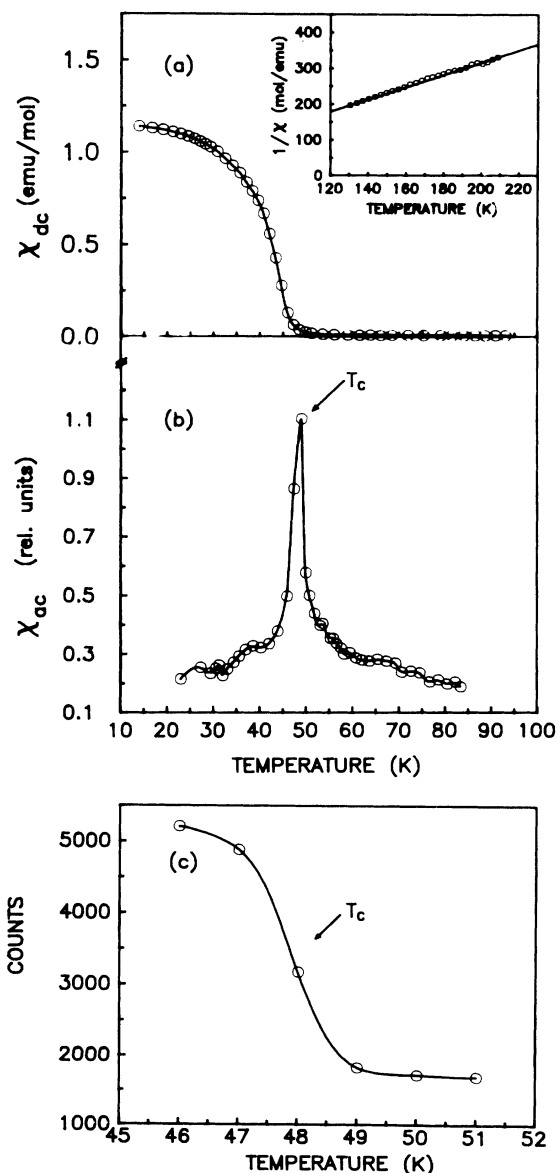


FIG. 5. (a) dc magnetization of NpSi_2 as function of temperatures at an applied magnetic field of 0.3 T. The reciprocal susceptibility data at elevated temperatures are inserted. (b) ac susceptibility for NpSi_2 as function of temperature. The sharp cusp indicates a ferromagnetic transition at $T_C = 48(2)$ K. (c) Determination of the ferromagnetic transition temperature T_C for NpSi_2 by Mössbauer thermal scan.

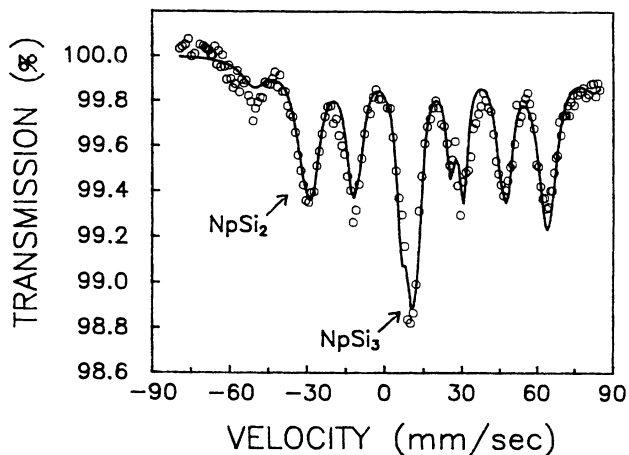


FIG. 6. ^{237}Np Mössbauer absorption spectrum of NpSi_2 at 4.2 K. A small amount of NpSi_3 is revealed by an unsplit absorption line at $\approx +11$ mm/sec.

ly shielded and thus contribute little additional density at the ^{237}Np nucleus. It is concluded that, in order to observe a significant IS in the metallic $3+$ region, the $5f$ -electron density must be strongly affected. This is possible by hybridization. We have shown recently that, by application of external hydrostatic pressure on metallic Np^{3+} compounds [e.g., NpSn_3 (Ref. 5)], hybridization can be increased decisively and the degree of the hybridization can be scaled to the volume dependencies of μ_{ord} , T_C and $\rho(0)$.⁵ In addition, under pressure, the change in the Mössbauer IS is always more negative [$\rho(0)$ increases] because $5f$ delocalization decreases the shielding of s electrons. We conclude that increasing hybridization in the Np^{3+} region must be associated with a more negative IS. This is the reason for comparing the NpX_2 systems according to their IS sequence (Table I) thus providing a measure of $5f$ - d - p - s band hybridization.

The principal component of the EFG tensor eq_z evaluated at the nucleus in noncubic symmetry originates mainly from $5f$ electrons.¹⁸ Together with the lattice field gradient, a noticeable quadrupole interaction should be expected, as actually found for many nonmetallic Np compounds. For the NpX_2 systems, however, no (or very small) quadrupole interaction is experimentally observed as shown in Table I. This hints that hybridization cancels, or partially suppresses, eq_z .

The discrepancy between μ_{ord} and μ_{sat} , which is present in all compounds investigated except for NpGa_2 (Table I), probably is another indication for the delocalization of $5f$ electrons. Recent relativistic calculations by Eriksson *et al.* utilizing local-spin-density (LSD) formalism¹⁷ showed that, by taking into account the conduction electron polarization, this discrepancy can be resolved. At present, such LSD calculations are available only for NpAl_2 and we shall further comment on this below.

In conclusion, anisotropic $5f$ -electron hybridization should affect all the Mössbauer hyperfine parameters, namely, the magnetic hyperfine field (and accordingly μ_{ord}), the quadrupole interaction, and the isomer shift. These parameters of the NpX_2 family are thus compared

TABLE I. Properties of NpX₂ intermetallics. The isomer shifts are the same above and below T_C and are given with respect to NpAl₂. NpF₃ is shifted +38 mm/sec relative to NpAl₂.

Compound	NpAl ₂	NpAs ₂	NpSi ₂	NpGa ₂	NpSb ₂	NpTe ₂
Isomer shift (mm/sec)	0	3	7.9	15.2	18	28
Hyperfine field B _{hf} (T)	330	319	244	525	424	≈0
Quadrupole int. e ² qQ (mm/sec)	≈0	+24	≈0	≈0	≈0	+12
T _C (K)	56	52/18	48	55	45	
Magnetic structure	F	AF/F	F	F	F	P
Ordered moment at 4.2 K (μ _B)	1.5	1.45	1.1	2.39	1.93	≈0
Saturation moment (μ _B)	1.38	1.32	0.8	2.4	1.3	
Paramagnetic moment (μ _B)	2.3	1.88	2.15	2.60	2.87	2.88
Crystallographic structure	Cubic laves <i>Fd3m</i>	Tetr. Fe ₂ As <i>P4/nmm</i>	Tetr. ThSi ₂ <i>I4₁/amd</i>	Hexa. AlB ₂ <i>P6/mmm</i>	Orto. LaSb ₂ ?	Tetr. Fe ₂ As <i>P4/nmm</i>
Np-Np spacing (Å)	3.37	3.96	3.92	4.08	?	4.42
References	24	22,23	This paper	This paper	23,27	23,27

in Table I.

NpSi₂ and NpGa₂ have isomer shifts in between NpAs₂ and NpSb₂. Within the Mössbauer IS systematics, the Np ion in these compounds should be classified as Np³⁺. If this assumption is correct, hybridization has to be significant since, as discussed above, it is mainly this mechanism that can cause the observed increase of the *s*-electron density at the Np nucleus when compared to the Np³⁺ ion in highly ionic compounds like, e.g., NpF₃. Most striking and surprising is the fact that a simple localized model of the crystalline electric field using a free-ion Russell-Saunders (RS) coupling reveals reasonable values for the ordered moments of a Np³⁺ ion in a large number of compounds.¹³ According to Hund's rule, the ground term of Np³⁺ (5*f*⁴) is ⁵I₄. In an ionic model, the ⁵I₄ state in a cubic CEF generally splits into a singlet Γ₁, a non-Kramer's doublet Γ₃, and two triplets Γ₄ and Γ₅.¹⁹ When lowering the symmetry, the degeneracies of the Γ₄ and the Γ₅ are lifted. Intermediate coupling usually improves the RS approximation, leading to correct values of the calculated order moments in a variety of 5*f* systems.^{20,21} This gave legitimization to the use of CEF models, which, by definition, apply to localized *f* electrons, in interpreting the magnetic properties of many actinide intermetallics.

Based on magnetic form-factor measurements, it has previously been suggested by Amoretti *et al.* that the ground state of NpAs₂ is probably Np³⁺ (⁵I₄).²⁰ At low temperatures, exchange splitting removes the degeneracy of the doublet Γ₅, leading to a calculated ordered moment of 1.5μ_B and an effective moment of 2.1μ_B (RS cou-

pling).^{13,20,21} These calculated values are surprisingly close to the experimental results.^{22,23} Further support of this picture comes from the observation of a rather significant quadrupole interaction. However, the low value of the observed saturation moment (μ_{sat}) of NpAs₂, in addition to the large IS relative to NpF₃, is not explained by this approach (Table I). Therefore, we believe that hybridization of the 5*f* electrons plays an important role also in this system.

As stated earlier, within the general systematics of the Np Mössbauer isomer shifts,¹² NpGa₂ should be considered a Np³⁺ (5*f*⁴) non-Kramer's ion with a ⁵I₄ Hund's-rule ground term. Assuming a free-ion Russell-Saunders coupling scheme for this ground state, an effective moment μ_{eff}=2.68μ_B and an ordered moment μ₀=2.4μ_B are calculated,^{13,21} in very good agreement with the experimental values. The magnetic hyperfine field is practically the free-ion value pointing to a highly localized (narrow-band) 5*f*-electron system. This approach is further supported by the value of the saturation moment which is close to that of the ordered moment (Table I). However, with respect to NpF₃, the Mössbauer IS is ≈23 mm/sec more negative, i.e., the *s*-electron density at the Np nucleus is higher and even more surprising, no quadrupole interaction is observed in NpGa₂. Both effects strongly indicated 5*f* hybridization in this compound, and thus the CEF levels are influenced by the hybridization dressing. According to Ref. 2, crystal-field dressing of hexagonal CEF will lead, for example, to admixture of the Γ₅ and Γ₆ symmetry bands with the appropriate local levels. This will push certain CEF levels

down in energy. But still, the ground state might be represented by an *effective* 5I_4 term.

The non-Curie-Weiss paramagnetic susceptibility below 110 K and the non-Brillouin-like behavior below T_C may be explained by temperature-dependent orthorhombic distortions associated with anisotropic hybridization. Similar distortions have previously been reported for the isostructural intermetallic UGa_2 .¹⁰

The IS of $NpSi_2$ (+7.9 mm/sec) lies in between $NpAs_2$ and $NpGa_2$, i.e., ≈ 30 mm/sec more negative than for NpF_3 . From the Zeeman split Mössbauer absorption pattern at 4 K and the susceptibility measurements, it is concluded that ferromagnetic order is established below 48 K. Again, negligible quadrupole interaction is observed, which, together with the negative value (as compared to $NpGa_2$) of the IS and the low μ_{ord} , gives a strong hint for severe $5f$ hybridization. Since Fig. 2 shows that saturation has been reached, the large discrepancy between μ_{ord} and μ_{sat} can by no means be described by a CEF model.

Even stronger hybridization is revealed in $NpAl_2$ if we assume that the Np ion has a formal Np^{3+} charge state. This assumption is in discrepancy with Ref. 24. For a non-Kramer's Np^{3+} ion in a Γ_5 doublet ground state, the calculated values of $\mu_{eff}=2.1\mu_B$ and $\mu_{ord}=1.5\mu_B$ are in close agreement with the experimental results given in Table I. In addition, the Mössbauer spectra under pressure at 4 K were successfully interpreted by assuming a relaxation process within a doublet and a singlet state²⁵ which supports a 5I_4 ground state. However, the discrepancy between the ordered moment μ_{ord} and the saturation moment μ_{sat} , together with the absence of a quadrupole interaction, is an indication that ionic models are not valid for $NpAl_2$. Again, we are driven to the conclusion that hybridization processes together with relativistic effects must be considered when analyzing the experimental data. The relativistic calculations by Eriksson *et al.* utilizing local-spin-density formalism²⁶ show that, by taking into account electronic pressure and conduction electron polarization, the discrepancy between the ordered moment μ_{ord} derived from Mössbauer and neutron-diffraction studies and the saturation moment μ_{sat} measured by dc magnetization (Table I), is justified. Unfortunately, in Ref. 26 no value for the isomer shift is given. This type of calculation, which we hope will be performed in the future for $NpAl_2$ as well as for other NpX_2 systems, should reproduce the magnetic moments, the quadrupole interaction, and the IS. At present, such LSD calculations are not available. As for $NpGa_2$, a

much simpler model invoking the CEF dressing can only give a qualitative description for the magnetic properties of $NpAl_2$.

The systematics of the Mössbauer IS also predicts that $NpSb_2$ is in a Np^{3+} (5I_4) ground state. The experimental values for the moments $\mu_{eff}=2.87\mu_B$ and $\mu_{ord}=1.9\mu_B$ (Refs. 13 and 27) are much too high to be explained within an ionic model for a Np^{3+} and too low for a Np^{4+} configuration.¹³ In addition, the discrepancy between the ordered moment and the saturation moment of $NpSb_2$ can definitely not be accounted for by CEF ionic models. Although the IS of $NpSb_2$ is close to that of $NpGa_2$, the magnetic hyperfine fields (ordered moments) as well as the saturation moments of these two compounds are quite different. Therefore, hybridization dressing of the CEF levels alone may not be sufficient to explain the properties of $NpSb_2$.

The IS of $NpTe_2$ is already rather close to that of NpF_3 and the Np ion is expected to be in the Np^{3+} ionic charge state,^{15,23,27} thus hybridization plays a minor role. $NpTe_2$ stays paramagnetic down to 1.2 K (Ref. 27) (Table I). This might be attributed to the large Np-Np separation where coupling between orbital moments is already rather weak. In the low-temperature limit $NpTe_2$ is expected to order magnetically. Further experiments are needed to test this prediction.

V. CONCLUSIONS

(a) The magnetic properties of $NpGa_2$ indicate a narrow $5f$ band whereas $NpSi_2$ hints partial $5f$ delocalization.

(b) All the investigated NpX_2 compounds, with the possible exception of $NpTe_2$, show the importance of $5f$ hybridization processes and relativistic effects in establishing their magnetic and hyperfine properties.

(c) Although CEF dressing turns out to be important, at present there exists no theoretical model which might explain consistently the magnetic moments μ_{ord} and μ_{sat} , as well as the IS and quadrupole interaction in the NpX_2 family.

ACKNOWLEDGMENTS

This work was funded by the German Federal Minister for Research and Technology (BMFT) under Contract Nos. 03-GALBEE, and 03KA2TUM-4 and by the National Council for Research and Development, Israel.

¹H. Hill, Nucl. Metall. **17**, 2 (1971).

²B. R. Cooper, J. M. Willis, N. Kioussis, and Q. G. Sheng, J. Phys. (Paris) Colloq. **49**, C8-463 (1988).

³P. M. Levy and S. Zhang, Phys. Rev. Lett. **62**, 78 (1989).

⁴J. Gal, F. J. Litterst, W. Potzel, J. Moser, U. Potzel, S. Fredo, S. Tapuchi, G. Shani, J. Jove, A. Cousson, M. Pages, and G. M. Kalvius, Phys. Rev. Lett. **21**, 2413 (1989).

⁵G. M. Kalvius, S. Zwirner, U. Potzel, J. Moser, W. Potzel, F. J. Litterst, J. Gal, S. Fredo, I. Yaar, and J. C. Spirlet, Phys.

Rev. Lett. **65**, 2290 (1990).

⁶R. Elliott and B. C. Giessen, Mater. Sci. Eng. **23**, 113 (1976).

⁷S. Tapuchi, Ph.D. thesis, Ben-Gurion University of the Negev, Beer-Sheva, Israel, 1988.

⁸J. Gal and J. Hess, Rev. Sci. Instrum. **42**, 543 (1971).

⁹I. Yaar, MSc. thesis, Ben-Gurion University of the Negev, Beer-Sheva, Israel, 1990.

¹⁰A. V. Andreev, K. P. Belov, A. V. Deriagin, Z. A. Zazei, R. Z. Levitin, A. Menkovsky, Yu. V. Popov, and V. I. Silant, Zh.

- Eksp. Teor. Fiz. **75**, 2351 (1978) [Sov. Phys. JETP **48**, 1187 (1978)].
- ¹¹A. V. Andreev, K. P. Belov, A. V. Deriagin, R. Z. Levitin, and A. Menkovsky, J. Phys. (Paris) Colloq. **40**, C4-82 (1979).
- ¹²A. C. Lawson, A. Williams, J. L. Smith, P. A. Seeger, J. A. Goldstone, J. A. O'Rourke, and Z. Fisk, J. Magn. Magn. Mater. **50**, 83 (1985).
- ¹³J. M. Fournier, in *Actinide-Chemistry and Physical Properties*, edited by L. Manes (Springer-Verlag, Berlin, 1985), p. 134.
- ¹⁴B. D. Dunlap and G. H. Lander, Phys. Rev. Lett. **33**, 1046 (1974).
- ¹⁵B. D. Dunlap and G. M. Kalvius, in *Handbook On The Physics And Chemistry Of The Actinides*, edited by A. J. Freeman and G. H. Lander (North-Holland, Amsterdam, 1985), Vol. 2, Chap. 5, p. 367.
- ¹⁶J. K. Jorgensen, R. Papporparado, and H. H. Schndlitke, J. Chem. Phys. **39**, 1422 (1963).
- ¹⁷Olle Eriksson, Ph.D. thesis, Uppsala University, 1989.
- ¹⁸A. J. Freeman and D. D. Koelling, in *Handbook On the Physics And Chemistry Of The Actinides*, edited by A. J. Freeman and J. B. Darby (North-Holland, Amsterdam, 1985), Vol. 1, Chap. 2, p. 384; see also B. D. Dunlap, G. M. Kalvius, and G. K. Shenoy, Phys. Rev. Lett. **26**, 1085 (1971).
- ¹⁹K. R. Lea, M. J. M. Leask, and W. P. Wolf, J. Phys. Chem. Solids **23**, 1381 (1962).
- ²⁰G. Amoretti, A. Blaise, M. Bonnet, J. X. Boucherle, A. Delapalm, J. M. Fournier, and F. Vigneron, J. Phys. (Paris) Colloq. **43**, C7-293 (1982).
- ²¹J. Gal, H. Pinto, S. Fredo, H. Shaked, W. Schäfer, G. Will, F. J. Litterst, W. Potzel, L. Asch, and G. M. Kalvius, Hyperfine Interact. **33**, 173 (1987).
- ²²A. Blaise, J. M. Fournier, D. Damien, A. Wojakowski, and J. P. Charvillat, J. Magn. Magn. Mater. **30**, 265 (1982).
- ²³M. Boge, J. Chappert, L. Asch, G. M. Kalvius, A. Blaise, J. M. Fournier, D. Damien, and A. Wojakowsky (unpublished).
- ²⁴F. J. Litterst, J. Moser, W. Potzel, U. Potzel, G. M. Kalvius, L. Asch, J. Gal, and J. C. Spirlet, Physica B **144**, 41 (1986).
- ²⁵F. J. Litterst, J. Moser, W. Potzel, U. Potzel, G. M. Kalvius, L. Asch, and J. Gal (unpublished).
- ²⁶O. Eriksson, B. Johansson, and M. S. S. Brooks, J. Phys. Condens. Matter. **2**, 1529 (1990).
- ²⁷A. Blaise, J. M. Fournier, D. Damien, and J. P. Charvillat, J. Magn. Magn. Mater. **29**, 297 (1982).